Giant Magnetoresistance without Defect Scattering

Kees M. Schep,[1,2] Paul J. Kelly,[1] Gerrit E. W. Bauer[2]

[1]*Philips Research Laboratories, Prof. Holstlaan 4, 5656 AA Eindhoven, The Netherlands*

[2]*Faculty of Applied Physics and Delft Institute for Microelectronics and Submicrontechnology, Delft University of Technology, Lorentzweg 1, 2628 CJ Delft, The Netherlands*

(Received 9 June 1994)

The ballistic transport properties of magnetic metallic multilayers are studied using calculations based on the local-spin-density approximation in which the *s* electrons and the *d* electrons, usually held responsible for conduction and magnetism, respectively, are treated on an equal footing. A giant magnetoresistance of up to 120% is calculated for point contacts of Co/Cu multilayers. The effect can be explained as a slowing down of the *s* electrons by hybridization with *d* electrons which are strongly reflected and partially localized by the spin-dependent interface potentials. The method should be a useful instrument in a systematic search for new materials for magnetoresistive applications.

PACS numbers: 71.25.Pi, 72.15.Gd, 73.40.Jn, 75.50.Rr

The giant magnetoresistance (GMR) effect in magnetic metallic multilayers has been the subject of intense investigation since its discovery only six years ago [1], mainly because of the advantages it promises for magnetic recording. There is consensus about the conditions under which the GMR effect occurs, namely, when the magnetizations of neighboring ferromagnetic layers, which are initially oriented antiparallel or at random, are aligned by applying an external magnetic field. A satisfactory microscopic explanation of the physical processes causing the GMR is still lacking, however. Most theories which attempt to explain the GMR by spin-dependent scattering at defects either in the bulk or at the interfaces do not treat the underlying electronic structure in a way which also describes the observed magnetic interlayer coupling. Instead, transport is assumed to be carried out by the *s* electrons, which are described by a parabolic band with some appropriate effective mass [2–11] or by a nondegenerate tight-binding band [12]. The magnetism, which is associated with the tightly bound *d* electrons, is introduced in terms of phenomenological scattering or tight-binding parameters. An important development is the recent measurement of GMR in the current-perpendicular-to-the-interface-plane (CPP) geometry [13–16] which not only results in an enhanced GMR but should also help to clarify the effect because of the higher symmetry and the clearer role of the interfaces as compared to the current-in-plane (CIP) geometry. In the following we will show that it should be even more instructive to extend these experiments into the ballistic regime.

The low-temperature electronic and magnetic properties of transition metals and transition metal multilayers are described very well by first-principles local-spin-density approximation calculations [17]. Two attempts to include realistic band structures into a theory of electronic transport in multilayers indicate that band structure effects may be important. Oguchi [18] examined the dependence of the Fermi velocities on the magnetic ordering. However, it is not clear under what conditions his relaxation time approximation with a phenomenological and constant scattering time is valid. Butler *et al.* [19] used the coherent potential approximation to model the interface roughness but their first-principles calculations predict unrealistically large effects, which may be due to the neglect of the vertex correction [20]. In the following we will identify a situation (i) where we can evaluate the MR rigorously and (ii) which is accessible to experiment. We will present the results of calculations for ballistic point contacts made from Co/Cu multilayers in the CIP and CPP geometries which demonstrate that a perfect, crystalline structure without any defects can support a giant MR. This contrasts with the common belief that GMR is mainly due to spin-dependent defect scattering. We will show that *s-d* hybridization, neglected in most current theoretical transport studies, is the all-important ingredient for ballistic GMR. Because our method is based on the full electronic structure, quantum interference and size effects are automatically included. These effects are known to be important from photoemission experiments [21] and from the experimental observations of the oscillatory variations of the interlayer coupling with both the nonmagnetic [22] and the magnetic [23] layer thickness and of the saturation resistance with the magnetic layer thickness [24].

We consider a multilayer structure where the total resistance is dominated by a classical point contact [25] with a diameter smaller than the mean free path and larger than the electron wavelength. Even though the electrons passing through the constriction are not scattered out of their Bloch states by defects, the conductance of the point contact is finite due to its finite cross section A. The spin-polarized ballistic (Sharvin) conductance G_σ for spin σ is simply the conductance quantum e^2/h times the number of conduction channels N_σ. N_σ is proportional to A and the projections $S_{\nu\sigma}$ of the Fermi surfaces for the different bands ν onto the plane normal

 0031-9007/95/74(4)/586(4)$06.00

to the transport direction $\hat{n}$:

$$G_\sigma(\hat{n}) = \frac{e^2}{h} N_\sigma = \frac{e^2}{h} \frac{A}{4\pi^2} \frac{1}{2} \sum_\nu S_{\nu\sigma}(\hat{n}) = \frac{e^2}{h} \frac{A}{4\pi^2} \frac{1}{2} \sum_\nu \int d\vec{q} |\hat{n} \cdot \vec{\nabla}_{\vec{q}} \varepsilon_{\nu\sigma}(\vec{q})| \delta(\varepsilon_{\nu\sigma}(\vec{q}) - E_F), \quad (1)$$

where $\varepsilon_{\nu\sigma}(\vec{q})$ are the energy bands. This formula has been derived using both the Boltzmann equation [26] and the Landauer-Büttiker formalism [27]. We note that in the absence of defect scattering the conductance is simply a Fermi surface property. Although present experiments on metallic multilayers are in the diffusive limit, the ballistic regime will be realized in future devices [28]. By making detailed predictions, we hope to stimulate more studies in this regime.

To evaluate Eq. (1) we calculated the band structures in the local-spin-density approximation using the linear muffin-tin orbital (LMTO) method in the atomic spheres approximation [29] in the parallel (P) and the antiparallel (AP) configurations for several (100) oriented Co_n/Cu_n multilayers. n is the number of atomic layers of each material in a unit cell which is repeated periodically in the growth direction. Results obtained for the (111) orientation are not much different. The in-plane lattice parameter was chosen to be that of bulk fcc copper; the cobalt layer was tetragonally distorted keeping the bond lengths constant. The charge and spin densities in the P configurations were calculated self-consistently using a basis of s, p, d, and f orbitals and a mesh of 1400 k points in the first Brillouin zone (BZ). From the self-consistent potentials the band structures were determined using an spd basis and different meshes containing up to 55 000 k points in the full BZ. The band structures in the AP configurations were calculated from potentials obtained by interchanging the spin densities from the corresponding P configuration on alternating Co_n/Cu_n cells. By calculating the potentials in the AP configuration for $n = 1, 2$ self-consistently, we checked that this has no influence on the final results. The projections of the Fermi surfaces were calculated using a suitable adaptation of the tetrahedron method [30].

Figures 1(a) and 1(b) show the projections of the Fermi surfaces in the CPP direction for the two spins of a (100) oriented Co_5/Cu_5 multilayer in the P configuration. The total shaded area is a measure of the conductance [31]. For a free electron material, the projection of the Fermi sphere is a circle which, in the presence of a periodic multilayer potential, splits up into a series of concentric rings separated by minigaps. The projection for the majority spin resembles the free electron projection but the circle is distorted in a way which reflects the fourfold symmetry of the underlying lattice. Near the edges of the BZ the gaps become wider because electrons that come in under grazing incidence with the interfaces can be reflected more easily. The projection for the minority spin is more difficult to interpret and certainly not free-electron-like, which is caused by the complicated Fermi surface for the Co minority spin. It is clear that the number of channels available for conduction is much smaller than for the majority spin. Some states (the thin lines) have no dispersion in the direction normal to the multilayer planes and can be identified as quantum well states. Because their velocity is perpendicular to $\hat{n}$, their contribution to the CPP transport is negligible. Figure 1(c) shows the projection of the Fermi surface of the same multilayer in the AP configuration. Because the projections for spin up and spin down electrons are identical, only one is shown. The number of gaps is twice as large for the AP configuration because the unit cell is doubled. The CPP-MR [MR = $(G_{P\uparrow} + G_{P\downarrow} - 2G_{AP})/2G_{AP}$] for this Co_5/Cu_5 multilayer is as high as 120%. Table I summarizes our results for layer thicknesses varying from $n = 1-8$. Small damped oscillations of the conductance as a function of the number of monolayers are observed for both spins in the AP configuration and for the P minority spin, reflecting the influence of quantum size effects on the conductance. For larger layer thicknesses the conductances saturate. We thus predict the surprising result that transport measurements in the ballistic regime will find values for the CPP-MR comparable to those measured in the diffusive limit. For the CPP geometry, the most important effect can be qualitatively cast in terms of a semiclassical model: the resistance for the minority spin channel in the P configuration is approximately equal to that of either channel in the AP configuration but is shunted by the "open" majority spin channel.

One conspicuous feature of Figs. 1(a)–(c) is the absence of (red) states with free-electron-like sp character. To understand the origin of the MR effect in the ballistic regime we investigated the influence of the hybridization between the d electrons and the free electrons in the sp band. We switched the sp-d hybridization off by setting the matrix elements between the sp and the d orbitals in the LMTO structure constants equal to zero. The band structures for the unhybridized situation were calculated using the same potentials as before. The resulting projection for the minority spin of the (100) oriented Co_5/Cu_5 multilayer in the P configuration is shown in Fig. 1(d). There is a striking difference compared with the hybridized situation of Fig. 1(b). The projections of the sp parts of the unhybridized Fermi surface are very free-electron-like, with only small distortions due to the fourfold rotational symmetry. Because the diameter of the circle is greater than the width of the first Brillouin zone the Fermi surface is folded back at the zone boundaries. The minigaps formed by the periodic multilayer potential appear quite clearly. The d states are confined to the magnetic layers and have no dispersion in the direction perpendicular to the multilayer plane. These quantum well states do not contribute to transport perpendicular to the interfaces. Similar results

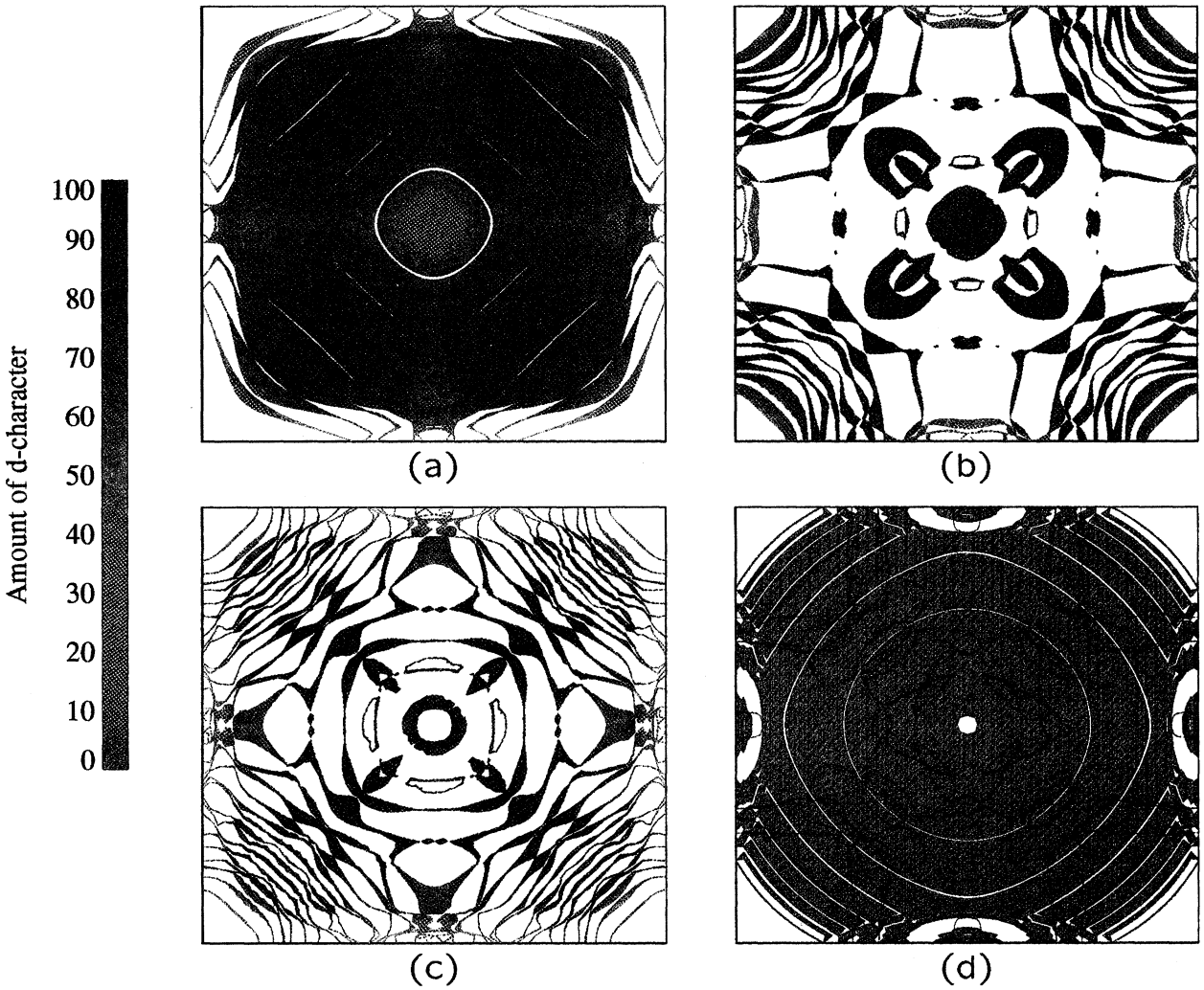

FIG. 1. Projections inside the first Brillouin zone of different Fermi surfaces for a (100) oriented Co_5/Cu_5 multilayer on a plane parallel to the interfaces. The amount of *d* character is given by the color code on the left-hand side of the figure. The Γ point is at the center of each panel. (a) Majority spin and (b) minority spin in the parallel configuration. (c) Either spin in the antiparallel configuration, (d) minority spin in the parallel configuration where the *sp-d* hybridization is omitted. The quantum well *d* states are just visible as thin blue lines.

were obtained for the majority spin and for the AP configuration. The MR decreases from 120% to 3% when the *sp-d* hybridization is neglected. This low value was already estimated from a simple model using realistic parameters [6]. The effect of the multilayer potential on the unhybridized free electrons is negligible. Hybridization with the *d* electrons results in strong coupling to the "magnetic lattice" and greatly enhanced reflection at the interfaces. GMR in the ballistic regime is thus induced by hybridization and theories that neglect this hybridization do not describe the effect correctly, at least not in this limit.

It would be very surprising if none of these band structure effects survived into the diffusive regime. For the CPP, in particular, the influence of the band structure is very important [10,12] and we find that the MR saturates at about 90% which is comparable with the experimental values obtained at low temperatures [14,16]. Thus, the CPP-MR can be explained by differences in the number of conduction channels only. Indeed, Asano *et al.* [12] have pointed out that, whereas the existence of MR in the CIP geometry depends critically on interface defect scattering, this is not true in the CPP geometry and so the results for the ballistic CPP-MR should be indicative for the experimental CPP-MR. The MR we calculated in the CIP geometry is only a few percent, indicating that some additional scattering mechanism is necessary to explain the experimentally observed value of 115% [32]. Still, we believe that the results derived in the ballistic limit have a more general significance. Spin-dependent surface roughness scattering is inextricably connected with the existence of strong spin-dependent reflection at the interfaces. To obtain GMR in the CIP geometry, both

TABLE I. Values of the calculated conductances G (in units of $10^{15}\ \Omega^{-1}\mathrm{m}^{-2}$) for several (100) oriented Co_n/Cu_n multilayers. $G_{P\uparrow}$ ($G_{P\downarrow}$): conductance of majority (minority) spin in the parallel configuration. G_{AP}: conductance per spin in the antiparallel configuration (both spins are the same). For comparison: the conductance per spin in copper is $0.55 \times 10^{15}\ \Omega^{-1}\mathrm{m}^{-2}$. The magnetoresistance is defined as $\mathrm{MR} = (G_{P\uparrow} + G_{P\downarrow} - 2G_{AP})/2G_{AP}$.

System	Co_1/Cu_1	Co_2/Cu_2	Co_3/Cu_3	Co_4/Cu_4	Co_5/Cu_5	Co_6/Cu_6	Co_7/Cu_7	Co_8/Cu_8
$G_{P\uparrow}$ (CPP)	0.51	0.45	0.45	0.43	0.43	0.42	0.42	0.42
$G_{P\downarrow}$ (CPP)	0.53	0.43	0.41	0.25	0.18	0.24	0.20	0.20
G_{AP} (CPP)	0.32	0.26	0.32	0.19	0.14	0.18	0.16	0.17
MR (CPP)	60%	71%	36%	78%	120%	86%	102%	78%
$G_{P\uparrow}$ (CIP)	0.46	0.53	0.50	0.50	0.49	0.48	0.49	0.50
$G_{P\downarrow}$ (CIP)	0.82	0.83	0.62	0.65	0.59	0.60	0.61	0.60
G_{AP} (CPP)	0.53	0.54	0.50	0.54	0.52	0.53	0.53	0.53
MR (CIP)	21%	25%	11%	6%	4%	3%	5%	3%

must be present. This means that a large CPP effect as calculated by the present method is a *necessary* condition for a GMR (either CPP or CIP), which makes it a promising instrument for materials research.

In summary, we have shown that in the ballistic limit the transport properties can be evaluated rigorously using parameter-free calculations based on the local-spin-density approximation. The calculated CPP-MR is comparable to experimental values, even though defect scattering has been completely disregarded. We hope that this will stimulate experimental studies of transport in multilayers in this regime. To describe the effect it is of crucial importance to take into account the complete hybridization. We emphasize that *no* empirical parameters or other phenomenological input have been used. The method should provide useful information on spin-dependent reflection at the interfaces of other materials.

We would like to thank Reinder Coehoorn and Martin Gijs for valuable discussions. One of the authors (G. E. W. B.) acknowledges support by the Stichting voor Fundamenteel Onderzoek der Materie (FOM).

[1] M. N. Baibich *et al.,* Phys. Rev. Lett. **61**, 2472 (1988); G. Binasch, P. Grünberg, F. Saurenbach, and W. Zinn, Phys. Rev. B **39**, 4828 (1989).
[2] R. E. Camley and J. Barnaś, Phys. Rev. Lett. **63**, 664 (1989).
[3] P. M. Levy, S. Zhang, and A. Fert, Phys. Rev. Lett. **65**, 1643 (1990).
[4] J. Inoue, A. Oguri, and S. Maekawa, J. Phys. Soc. Jpn. **60**, 376 (1991).
[5] S. Zhang and P. M. Levy, J. Appl. Phys. **69**, 4786 (1991).
[6] G. E. W. Bauer, Phys. Rev. Lett. **69**, 1676 (1992).
[7] R. Q. Hood and L. M. Falicov, Phys. Rev. B **46**, 8287 (1992); R. Q. Hood, L. M. Falicov, and D. R. Penn, Phys. Rev. B **49**, 368 (1994).
[8] P. B. Visscher and H. Zhang, Phys. Rev. B **48**, 6672 (1993); P. B. Visscher, Phys. Rev. B **49**, 3907 (1994).
[9] T. Valet and A. Fert, Phys. Rev. B **48**, 7099 (1993).
[10] S. Zhang and P. M. Levy, Mater. Res. Soc. Symp. Proc. **313**, 53 (1993).
[11] A. Brataas and G. E. W. Bauer, Europhys. Lett. **26**, 117 (1994).
[12] Y. Asano, A. Oguri, and S. Maekawa, Phys. Rev. B **48**, 6192 (1993); (private communication).
[13] W. P. Pratt, Jr. *et al.,* Phys. Rev. Lett. **66**, 3060 (1991).
[14] W. P. Pratt, Jr. *et al.,* J. Magn. Magn. Mater. **126**, 406 (1993).
[15] M. A. M. Gijs, S. K. J. Lenczowski, and J. B. Giesbers, Phys. Rev. Lett. **70**, 3343 (1993).
[16] M. A. M. Gijs *et al.,* J. Appl. Phys. **75**, 6709 (1994).
[17] M. van Schilfgaarde and F. Herman, Phys. Rev. Lett. **71**, 1923 (1993); P. Lang, L. Nordström, R. Zeller, and P. H. Dederichs, Phys. Rev. Lett. **71**, 1927 (1993); G. H. O. Daalderop, P. J. Kelly, and M. F. H. Schuurmans, in *Ultrathin Magnetic Structures I,* edited by J. A. C. Bland and B. Heinrich (Springer-Verlag, Berlin, 1994).
[18] T. Oguchi, J. Magn. Magn. Mater. **126**, 519 (1993).
[19] W. H. Butler, J. M. MacLaren, and X.-G. Zhang, Mater. Res. Soc. Symp. Proc. **313**, 59 (1993).
[20] J. C. Swihart, W. H. Butler, G. M. Stocks, D. M. Nicholson, and R. C. Ward, Phys. Rev. Lett. **57**, 1181 (1986).
[21] J. E. Ortega and F. J. Himpsel, Phys. Rev. Lett. **69**, 844 (1992).
[22] S. S. P. Parkin, N. More, and K. P. Roche, Phys. Rev. Lett. **64**, 2304 (1990); S. S. P. Parkin, Phys. Rev. Lett. **67**, 3598 (1991).
[23] P. J. H. Bloemen *et al.,* Phys. Rev. Lett. **72**, 764 (1994).
[24] S. N. Okuno and K. Inomata, Phys. Rev. Lett. **72**, 1553 (1994).
[25] Yu. V. Sharvin, Zh. Eksp. Teor. Fiz. **48**, 984 (1965) [Sov. Phys. JETP **21**, 655 (1965)].
[26] G. Wexler, Proc. Phys. Soc. **89**, 927 (1966).
[27] G. E. W. Bauer, A. Brataas, K. M. Schep, and P. J. Kelly, J. Appl. Phys. **75**, 6704 (1994).
[28] P. A. M. Holweg *et al.,* Phys. Rev. Lett. **67**, 2549 (1991).
[29] O. K. Andersen, Phys. Rev. B **12**, 3060 (1975).
[30] O. Jepsen and O. K. Andersen, Phys. Rev. B **29**, 5965 (1984).
[31] Different sheets of Fermi surface might be projected on top of each other and this is not visible in the figure. It is taken into account in the numerical results.
[32] S. S. P. Parkin, Z. G. Li, and D. J. Smith, Appl. Phys. Lett. **58**, 2710 (1991).

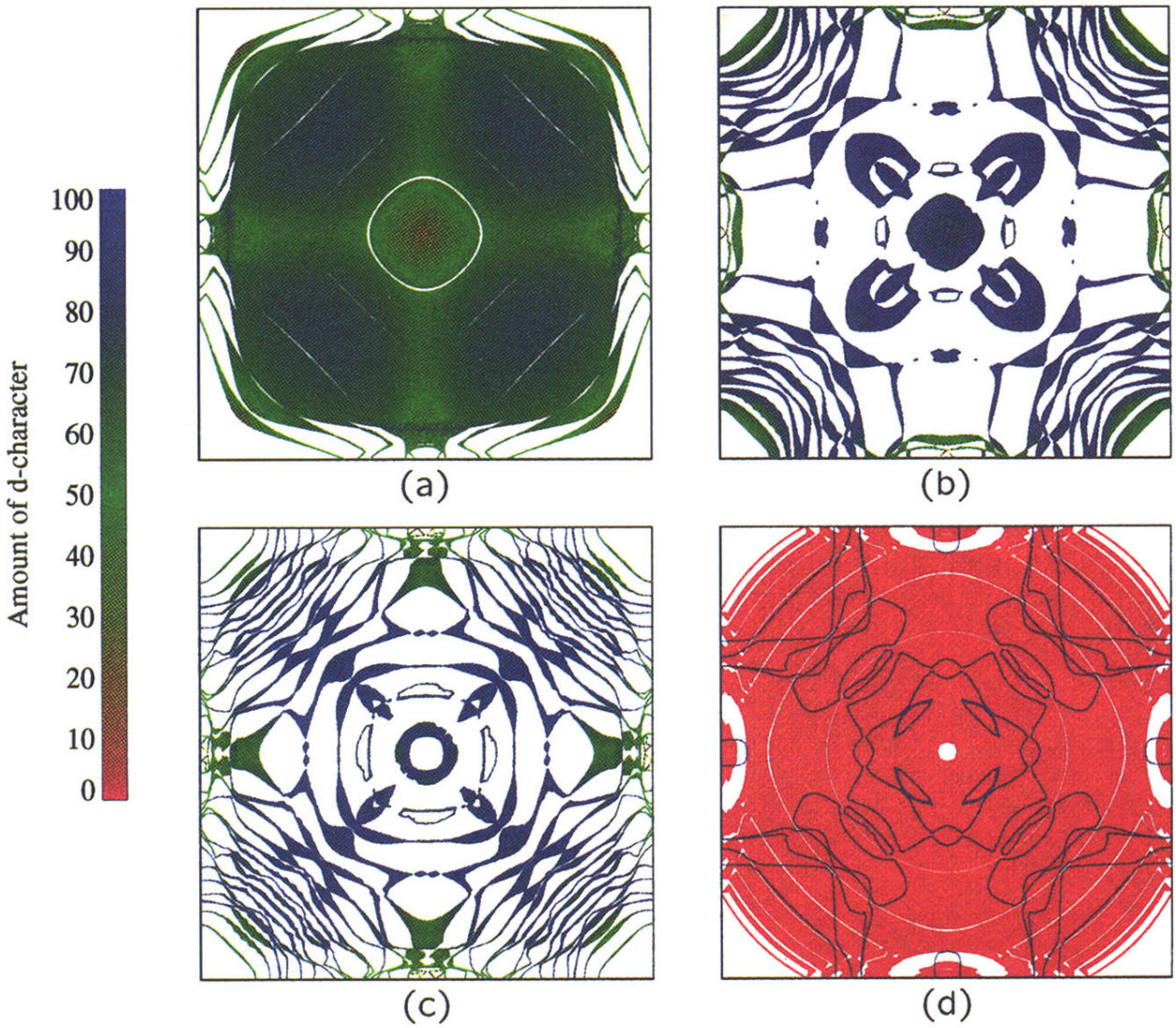

FIG. 1. Projections inside the first Brillouin zone of different Fermi surfaces for a (100) oriented Co_5/Cu_5 multilayer on a plane parallel to the interfaces. The amount of *d* character is given by the color code on the left-hand side of the figure. The Γ point is at the center of each panel. (a) Majority spin and (b) minority spin in the parallel configuration. (c) Either spin in the antiparallel configuration, (d) minority spin in the parallel configuration where the *sp-d* hybridization is omitted. The quantum well *d* states are just visible as thin blue lines.